Distributed Measurement-based Optimal DER Dispatch with Estimated Sensitivity Models

Severin Nowak, *Student Member, IEEE,* Yu Christine Chen, *Member, IEEE,* and Liwei Wang, *Member, IEEE*

***Abstract*—This paper presents a distributed measurement-based method to determine distributed energy resource (DER) active- and reactive-power setpoints that minimize bus voltage deviations from prescribed references, bus active- and reactive-power deviations from desired values, as well as cost of DER outputs. The proposed method partitions the system into multiple areas and performs per-area computations in parallel, thus mitigating scalability concerns of centralized implementations. A linear sensitivity model for each area is first estimated from measurements via the recursive weighted partial least-squares algorithm. The estimated sensitivity models are then embedded in an optimization problem, the structure of which is amenable to decomposition into per-area subproblems. The subproblems are solved in parallel using consensus-based alternating direction method of multipliers to obtain optimal DER setpoints. Both the estimation and optimization tasks require only the exchange of information at boundary buses among adjacent areas. Numerical simulations involving the IEEE 33-bus distribution test system illustrate the ability of the proposed method to determine optimal DER setpoints that adapt to operating-point changes in a distributed fashion. Additional numerical simulations involving the IEEE 123-bus system demonstrate computational scalability and the application to multi-phase systems in a practical scenario.**

***Index Terms*—Distributed energy resources, distributed model estimation, distributed optimization, optimal DER dispatch, partial least-squares estimation, phasor measurement units.**

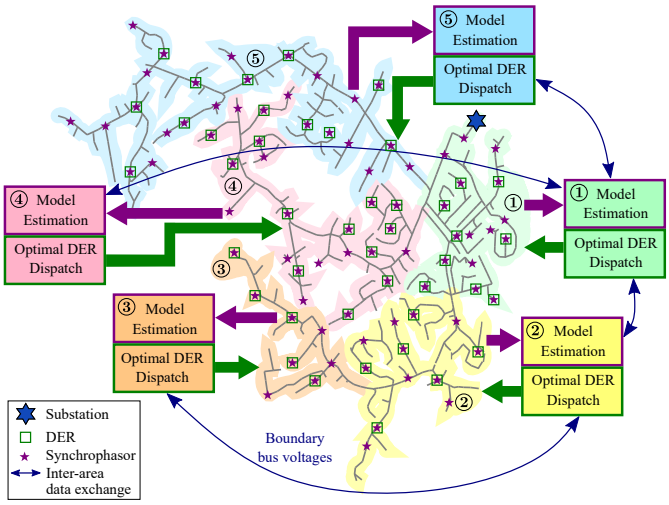

Fig. 1: Illustrating the proposed framework. The distribution system is partitioned into multiple areas. Each estimates its own per-area sensitivity model from synchrophasor measurements and subsequently solves its own optimal DER dispatch subproblem. The optimal DER setpoints are obtained with exchange of only boundary bus voltages via consensus-based alternating direction method of multipliers.

I. Introduction

MASSIVE deployment of distribution-level distributed energy resources (DERs), such as rooftop solar-photovoltaic, wind, and battery-storage systems, is crucial in the transition to a more sustainable energy future. These technologies have seen tremendous global growth in recent years. For example, today, the total installed capacity of small-scale solar-photovoltaic systems exceeds 20 GW in the United States and 7 GW in Australia [1]. Benefits for grid operations are undeniable when DERs can be suitably dispatched via online optimization routines [2]. However, optimal DER dispatch may be compromised by inaccurate offline network models due to incorrect topology information and fast-changing operating points, resulting in suboptimal or undesired system behaviours [3]. Recent research provides promising directions in measurement-based methods to infer up-to-date information about pertinent properties like voltage sensitivities [4], the power-flow Jacobian matrix [5], and network topology [6]. The ability to accurately estimate up-to-date system attributes motivates widespread installations of measurement equipment in distribution grids [7]. Particularly, distribution-level phasor measurement units are well-suited for online optimization, as they record so-called *synchrophasors*—time-synchronized measurements of voltage and current phasors—with phase angle accuracy of $0.01°$; and they transmit the data at intervals in the sub-second range through a standardized communication interface (e.g., IEEE C37.118) [3]. In the future, synchrophasor technology is expected to be embedded in devices like inverter-interfaced DERs, transformers, and protection relays, leading to significantly expanded metering capability in distribution systems [7]. With the vast synchrophasor data volume and greater DER integration, however, estimation of relevant attributes and the ensuing optimal DER dispatch become large-scale problems with many decision variables, which poses challenges for effective and timely DER dispatch.

Aimed at practical implementation and scalability, we propose a measurement-based *and* distributed approach to determine DER active- and reactive-power setpoints that regulate bus voltages and power injections while minimizing cost of DER outputs. Figure 1 provides an illustration of the proposed framework, which consists of two successive and iterative stages: (i) estimating sensitivity models, and (ii)

Severin Nowak is with the Lucerne University of Applied Sciences and Arts, Lucerne, Switzerland. E-mail: severin.nowak@hslu.ch. Yu Christine Chen is with the Department of Electrical and Computer Engineering at The University of British Columbia, Vancouver, Canada. E-mail: chen@ece.ubc.ca. Liwei Wang is with the School of Engineering at The University of British Columbia, Okanagan Campus, Kelowna, Canada. E-mail: liwei.wang@ubc.ca. This work was supported by Mitacs through the Mitacs Accelerate program with industrial partner Enbala Power Networks Inc.

optimizing DER setpoints. In the estimation stage, we partition the system into multiple areas and, instead of relying on an accurate offline model, we estimate a linear voltage-to-power sensitivity model for each area using synchrophasor measurements available at (possibly a subset of) buses therein. Then, in the second stage, we embed the estimated sensitivity models from all areas as equality constraints into a convex quadratic optimization problem. Per-area sensitivity models are crucial to enable decomposition of the optimization into per-area subproblems that can then be solved, in parallel fashion, via consensus-based alternating direction method of multipliers (ADMM) to reach an optimal operating point for the entire system. The per-area estimation and optimization tasks exchange pertinent information for only boundary buses among adjacent areas.

We focus our review of prior art in the domains of distributed estimation and measurement-based optimal DER dispatch. Distributed algorithms are of particular interest for large-scale distribution networks in order to improve scalability and data privacy. For example, the problem of distributed power system state estimation is addressed via consensus-based ADMM in [8], distributed semidefinite programming in [9], and more recently, a distributed gradient-based method in [10]. Shifting attention to measurement-based optimal DER dispatch, [11] uses rule- and optimization-based control strategies in conjunction with an estimated second-order power-flow sensitivity model. Furthermore, [12], [13] leverage estimated power-to-voltage sensitivities to determine DER setpoints that regulate voltages or substation injection with prior knowledge of feasible topological configurations. In contrast, model-free control via an extremum seeking approach is developed in [14]. It forgoes the use of a network model by actively probing the grid with sinusoidal perturbations of DER injections. Our previous work in [15] estimates a voltage-to-power sensitivity model and embeds it in an optimization problem to dispatch DERs toward multiple operational objectives. However, the measurement-based DER dispatch methods reviewed above all involve centralized optimization, which may be computationally expensive for large distribution networks with many DERs and measurements. To avoid potential scalability issues of centralized methods, distributed feedback-based optimization adjusts DER setpoints recursively to converge to the optimal operating point using measurements as the feedback signal. Optimal voltage control has been implemented in distributed fashion via feedback-based optimization [16]–[18]. Primal-dual gradient methods solving a saddle-point problem achieve combined regulation of substation power supply and system voltage levels in [2], [19]. These methods tend to be robust against variations in loads and renewable generation [20], and they can cope with inaccuracies in the network model. Nevertheless, in order to compute pertinent gradients in the feedback-based optimization methods, prior knowledge of the network topology and line parameters is required.

In this paper, we develop a *distributed measurement-based* approach to determine DER active- and reactive-power setpoints. We partition the network into multiple areas, and each area performs its own sensitivity model estimation and optimal DER dispatch in parallel. The estimation of per-area sensitivity models accommodates full or partial coverage of measurements available at all buses or a subset thereof, respectively. The key advantage of per-area estimation is that the number of estimated sensitivities is greatly reduced as compared with the full-network analogue. In the optimal DER dispatch stage, the distributed ADMM-based solution algorithm affords closed-form solutions in each subproblem. With respect to information related to the physical network, compared to [2], [16]–[19] that rely on some prior knowledge of the network topology and line parameters, each per-area subproblem in the proposed method requires only knowledge of which areas are adjacent to its boundary buses. Furthermore, we minimize the combined objective of regulating system voltages and power injections as well as minimizing cost of DER outputs, unlike [11]–[13], [16]–[18], which focus either on voltage regulation *or* active power provision. Also, compared with [14], the proposed method affords lower injection perturbations and temporal measurement resolution. Numerical simulations involving the IEEE 33-bus system demonstrate the effectiveness and adaptability of the proposed distributed measurement-based framework. Further simulations of the multi-phase IEEE 123-bus system with realistic load and renewable generation profiles demonstrate practical applicability and scalability. With the above in mind, this paper extends our previous work in [15] in two major directions: (i) estimation of per-area sensitivity models and (ii) distributed optimal DER dispatch, both of which are performed in parallel amongst different areas. We also demonstrate several nontrivial benefits of the proposed method via numerical simulations involving the IEEE 123-bus multi-phase test system. First, the proposed distributed approach accommodates larger and multi-phase systems with greater synchrophasor measurement coverage (the method in [15] suffers scalability limitations beyond 100 measured nodes) while reducing computation time and thus enhancing algorithmic scalability. Furthermore, it improves estimation accuracy since the per-area sensitivity model estimation avoids degradation of accuracy due to estimating zero entries. Finally, it does not compromise on optimality as the decomposed distributed optimization problem is equivalent to the original centralized one.

The remainder of this paper is organized as follows. Section II outlines the distribution network model and motivates the need for a distributed measurement-based approach. Section III presents the estimation of per-area sensitivity models. In Section IV, we formulate the distributed optimal DER dispatch problem with the estimated sensitivity models and subsequently solve it via consensus-based ADMM. Numerical simulations in Section V demonstrate the effectiveness and scalability of the proposed distributed DER dispatch framework. Finally, we provide concluding remarks in Section VI.

II. Preliminaries

In this section, we establish the system model and formulate the standard optimal DER dispatch problem. We also motivate the need for a distributed measurement-based approach.

A. Network and Power-flow Models

Consider a multi-phase distribution system with buses collected in the set $\mathcal{N} = \{1, \ldots, |\mathcal{N}|\}$. Suppose pertinent system variables are sampled at time $t = k\Delta t$, $k = 0, 1, \ldots$, where Δt is the sampling interval. We collect phases found at bus $i \in \mathcal{N}$ in the set $\mathcal{P}_i \subseteq \{a, b, c\}$. Let $V^{\phi}_{i,[k]}$ and $\theta^{\phi}_{i,[k]}$ denote, respectively, the magnitude and phase-angle of the line-to-neutral[1] voltage at bus $i \in \mathcal{N}$ in phase $\phi \in \mathcal{P}_i$, and at discrete time step k. Also let $P^{\phi}_{i,[k]}$ and $Q^{\phi}_{i,[k]}$ denote, respectively, the net active- and reactive-power injections at bus $i \in \mathcal{N}$ in phase $\phi \in \mathcal{P}_i$, and at time step k. Further collect multi-phase voltage phase-angles and magnitudes at all buses at time step k in vector $x_{[k]} = [\{\theta^{\phi}_{i,[k]}\}_{\phi\in\mathcal{P}_i, i\in\mathcal{N}}, \{V^{\phi}_{i,[k]}\}_{\phi\in\mathcal{P}_i, i\in\mathcal{N}}]^{\mathrm{T}}$. Analogously, collect multi-phase net active- and reactive-power injections at all buses at time step k in vector $y_{[k]} = [\{P^{\phi}_{i,[k]}\}_{\phi\in\mathcal{P}_i, i\in\mathcal{N}}, \{Q^{\phi}_{i,[k]}\}_{\phi\in\mathcal{P}_i, i\in\mathcal{N}}]^{\mathrm{T}}$. With the notation established above, the power-flow solution at time step k can be compactly expressed as $y_{[k]} = g(x_{[k]})$ where $g : \mathbb{R}^{2N^{\phi}} \to \mathbb{R}^{2N^{\phi}}$, with $N^{\phi} = \sum_{i\in\mathcal{N}} |\mathcal{P}_i|$. The dependence on network parameters (such as circuit breaker status and line impedances) is implicitly considered in the function $g(\cdot)$. In the neighbourhood sufficiently close to the operating point at time step k, the power-flow solution at the next time step $k+1$ can be approximated with the following linear sensitivity model:

$$y_{[k+1]} \approx J_{[k]} x_{[k+1]} + c_{[k]}, \tag{1}$$

where $J_{[k]}$ and $c_{[k]}$ respectively given by

$$J_{[k]} = \frac{dg}{dx}\Big|_{x_{[k]}}, \quad c_{[k]} = y_{[k]} - \frac{dg}{dx}\Big|_{x_{[k]}} x_{[k]},$$

are the linear- and constant-term coefficients evaluated at the operating point at time step k. It is worth noting that $J_{[k]}$ is a sparse matrix whose structure is intimately related to the network topology. This aspect is key to formulating distributed estimation and optimization problems in Sections III and IV, respectively.

B. Optimal DER Dispatch Problem

An optimal DER dispatch problem can be formulated to minimize a desired cost function (e.g., cost of DER outputs, deviations from reference values, etc.) subject to the linear sensitivity model in (1) and other operational constraints. To this end, let $\mathcal{D} \subset \mathcal{N}$ denote the set of buses connected to controllable DERs, and let $D^{\phi} = \sum_{i\in\mathcal{D}} |\mathcal{P}_i|$. Assume that the controllable DER at bus $i \in \mathcal{D}$ can inject nonzero active and reactive power into phase $\phi \in \mathcal{P}_i$. Denote by $P^{\phi,\mathrm{gen}}_{i,[k]}$ and $Q^{\phi,\mathrm{gen}}_{i,[k]}$, respectively, the controllable components of the active- and reactive-power injections in phase $\phi \in \mathcal{P}_i$ at bus $i \in \mathcal{D}$ and at time step k; and further collect these in vector $y^{\mathrm{gen}}_{[k]} = [\{P^{\phi,\mathrm{gen}}_{i,[k]}\}_{\phi\in\mathcal{P}_i, i\in\mathcal{D}}, \{Q^{\phi,\mathrm{gen}}_{i,[k]}\}_{\phi\in\mathcal{P}_i, i\in\mathcal{D}}]^{\mathrm{T}}$. Also collect the uncontrollable active- and reactive-power injections (arising from, e.g., loads) at all buses in vector $y^{\mathrm{load}}_{[k]} \in \mathbb{R}^{2N^{\phi}}$ so that $y_{[k]} = C y^{\mathrm{gen}}_{[k]} - y^{\mathrm{load}}_{[k]}$, where $C \in \mathbb{R}^{2N^{\phi}\times 2D^{\phi}}$ is the matrix that maps the DER bus/phase indices to buses/phases collected in the entire distribution network. Particularly, the entry in the ith row and jth column of C is 1 if the jth element of $y^{\mathrm{gen}}_{[k]}$ represents the same phase and bus as the ith element of $y_{[k]}$, and it is 0 otherwise. Then we formulate the following optimization problem to dispatch controllable DERs in the distribution network at time step $k+1$:

$$\underset{x_{[k+1]}, y_{[k+1]}, y^{\mathrm{gen}}_{[k+1]}}{\text{minimize}} \quad f(x_{[k+1]}, y_{[k+1]}, y^{\mathrm{gen}}_{[k+1]}), \tag{2a}$$

$$\text{subject to} \quad y_{[k+1]} = J_{[k]} x_{[k+1]} + c_{[k]}, \tag{2b}$$

$$y_{[k+1]} = y_{[k]} + C(y^{\mathrm{gen}}_{[k+1]} - y^{\mathrm{gen}}_{[k]}), \tag{2c}$$

$$x_{\min} \le x_{[k+1]} \le x_{\max}, \tag{2d}$$

$$y^{\mathrm{gen}}_{[k+1]} \in \mathcal{Y}^{\mathrm{gen}}, \tag{2e}$$

where $f : \mathbb{R}^{2N^{\phi}} \times \mathbb{R}^{2N^{\phi}} \times \mathbb{R}^{2D^{\phi}} \to \mathbb{R}$ is the cost to be minimized, $x_{\min}$ and $x_{\max}$ represent, respectively, the minimum and maximum limits of voltage phase-angles and magnitudes, and $\mathcal{Y}^{\mathrm{gen}}$ represents the allowable space of DER outputs [15]. Under typical DER control schemes (including, e.g., active-power control, reactive-power control, and joint active- and reactive-power control), $\mathcal{Y}^{\mathrm{gen}}$ is a convex set [2]. The underlying assumption for (2b) to hold is that $J_{[k]}$ and $c_{[k]}$ computed or estimated at time step k model the relationship between $y_{[k+1]}$ and $x_{[k+1]}$ at time step $k+1$ with sufficient accuracy. The constraint in (2c) holds under the assumption that the uncontrollable active- and reactive-power injections do not change significantly between time steps k and $k+1$. Nevertheless, we emphasize that any such fluctuations would be captured by the sensitivity model updated at the next time step $k+1$.

C. Problem Statement

In [15], we developed a measurement-based method that leverages synchrophasor measurements at a subset of buses to estimate a reduced version of the sensitivity model in (1); and both the model estimation and optimal DER dispatch steps are solved in *centralized* fashion. Numerical case studies demonstrate that execution times are feasible for real-time implementation with relatively few measurements and DERs in the network [15]. However, with the projected vast deployments of DERs and synchrophasor measurements in multi-phase distribution systems [1], [7], the centralized method involves large-scale estimation and optimization problems that are computationally burdensome for real-time field implementations. To avoid potential scalability issues, in this paper, we partition the distribution system into multiple areas, each consisting of a portion of the full network. We estimate a linear sensitivity model for each area and further solve the optimal DER dispatch problem in a *distributed* manner, enabled by consensus-based ADMM. The proposed distributed measurement-based method has several key advantages: (i) it reduces the computational burden in both the model estimation and optimal DER dispatch tasks, (ii) it readily adapts to operating-point changes by estimating per-area sensitivity models online, and (iii) it affords greater data privacy as measurements, cost function, and operational constraints are only shared within the area.

[1]Delta connections can be converted to wye connections in accordance with our notation.

III. Per-area Sensitivity Model Estimation

In this section, we estimate the linear sensitivity model relating measured bus voltages to power injections for each area in the distribution network.

A. Problem Formulation

We partition the distribution network into non-overlapping areas collected in the set $\mathcal{A}$. Within area $\alpha \in \mathcal{A}$, buses with synchrophasor measurements are collected in the set $\mathcal{E}^\alpha$, and those connected to DERs, whose setpoints can be remotely updated, are collected in $\mathcal{D}^\alpha$. The formulation is general in the sense that it accommodates synchrophasor measurements collected at a subset of buses or at all buses within an area. For distinct areas $\alpha, \gamma \in \mathcal{A}$, $\mathcal{E}^\alpha \cap \mathcal{E}^\gamma = \emptyset$. Furthermore, let $\mathcal{E}^{\alpha+}$ represent the *extended* set of buses in each area $\alpha \in \mathcal{A}$, which also collects the one-hop adjacent measured buses belonging to areas adjacent to area α. Denote the set of adjacent areas of area α by $\mathcal{A}^\alpha$, and boundary buses for area α are collected in $\mathcal{B}^\alpha = \cup_{\gamma \in \mathcal{A}^\alpha}(\mathcal{E}^{\alpha+} \cap \mathcal{E}^{\gamma+})$. Let $\mathcal{A}_i = \{\alpha, i \in \mathcal{E}^{\alpha+}\}$ comprise areas for which the extended set of buses contains bus i.

Denote the measured voltage phase-angle and magnitude at bus i in phase ϕ at time step k as $\widehat{\theta}^\phi_{i,[k]}$ and $\widehat{V}^\phi_{i,[k]}$, respectively. Similarly, let $\widehat{P}^\phi_{i,[k]}$ and $\widehat{Q}^\phi_{i,[k]}$ denote the measured net active- and reactive-power injections at bus i in phase ϕ at time step k. Collect measured quantities pertinent to area $\alpha \in \mathcal{A}$ in vectors $\widehat{x}^\alpha_{[k]} = [\{\widehat{\theta}^\phi_{i,[k]}\}_{\phi \in \mathcal{P}_i, i \in \mathcal{E}^{\alpha+}}, \{\widehat{V}^\phi_{i,[k]}\}_{\phi \in \mathcal{P}_i, i \in \mathcal{E}^{\alpha+}}]^{\mathrm{T}}$ and $\widehat{y}^\alpha_{[k]} = [\{\widehat{P}^\phi_{i,[k]}\}_{\phi \in \mathcal{P}_i, i \in \mathcal{E}^{\alpha}}, \{\widehat{Q}^\phi_{i,[k]}\}_{\phi \in \mathcal{P}_i, i \in \mathcal{E}^{\alpha}}]^{\mathrm{T}}$. Further hypothesizing that, for area $\alpha \in \mathcal{A}$, the active- and reactive-power injections are linearly related to bus-voltage phase-angles and magnitudes, we get

$$\widehat{y}^\alpha_{[k]} = J^\alpha_{[k]} \widehat{x}^\alpha_{[k]} + c^\alpha_{[k]},\ \alpha \in \mathcal{A}, \tag{3}$$

where $J^\alpha_{[k]}$ and $c^\alpha_{[k]}$ form the sensitivity model relating measured voltages to power injections in area $\alpha \in \mathcal{A}$. Note that, in (3), while $\widehat{x}^\alpha_{[k]}$ includes voltage magnitudes and angles at one-hop adjacent buses in adjacent areas, $\widehat{y}^\alpha_{[k]}$ includes power injections at only buses within area α. This is because we are interested in the sensitivity of bus injections in a particular area to the voltages on adjacent buses, which includes the one-hop adjacent buses in adjacent areas. With the voltage measurements at the one-hop adjacent buses in adjacent areas included in (3), the structure of the distribution network admittance matrix enables the estimation of per-area sensitivities without compromising the accuracy. Then, there exists $H^\alpha_{[k]}$ that satisfies the relationship:

$$(\widehat{y}^\alpha_{[k]})^{\mathrm{T}} = \begin{bmatrix} (\widehat{x}^\alpha_{[k]})^{\mathrm{T}} & 1 \end{bmatrix} H^\alpha_{[k]},\ \alpha \in \mathcal{A}, \tag{4}$$

where $H^\alpha_{[k]} = [J^\alpha_{[k]}, c^\alpha_{[k]}]^{\mathrm{T}}$. In the per-area estimation, our goal is to evaluate the entries of $H^\alpha_{[k]}$ for each area $\alpha \in \mathcal{A}$ based on measurements pertinent to the area.

B. Solution Algorithm

In order to improve adaptability to operating-point changes and to reduce computational burden, we estimate the entries of $H^\alpha_{[k]}$ using only online synchrophasor measurements pertinent to area α and one-hop adjacent buses belonging to adjacent areas of area α. To this end, suppose that M samples of voltage phase-angles and magnitudes, $\widehat{x}^\alpha_{[k-M+1]}, \ldots, \widehat{x}^\alpha_{[k]}$, and active- and reactive-power injections, $\widehat{y}^\alpha_{[k-M+1]}, \ldots, \widehat{y}^\alpha_{[k]}$, are available. Also, assume that the operating point remains approximately constant over the M measurement samples (we will remove this assumption later). Then, with $M > 2|\mathcal{E}^\alpha|$, we collect M instances of (4) to form the subsequent over-determined system of linear equations:

$$Y^\alpha_{[k]} = X^\alpha_{[k]} H^\alpha_{[k]},\ \alpha \in \mathcal{A}, \tag{5}$$

where $X^\alpha_{[k]}$ and $Y^\alpha_{[k]}$ are given by

$$X^\alpha_{[k]} = \begin{bmatrix} (\widehat{x}^\alpha_{[k-M+1]})^{\mathrm{T}} & 1 \\ \vdots & \vdots \\ (\widehat{x}^\alpha_{[k]})^{\mathrm{T}} & 1 \end{bmatrix}, \quad Y^\alpha_{[k]} = \begin{bmatrix} (\widehat{y}^\alpha_{[k-M+1]})^{\mathrm{T}} \\ \vdots \\ (\widehat{y}^\alpha_{[k]})^{\mathrm{T}} \end{bmatrix}. \tag{6}$$

Since (5) is over-determined, we can obtain the ordinary least-squares (OLS) estimate for $H^\alpha_{[k]}$ as

$$\widehat{H}^\alpha_{[k]} \approx ((X^\alpha_{[k]})^{\mathrm{T}} X^\alpha_{[k]})^{-1} (X^\alpha_{[k]})^{\mathrm{T}} Y^\alpha_{[k]}. \tag{7}$$

In practice, however, similar patterns in voltage phase-angle and magnitude measurements at different buses due to changing operating points may challenge the OLS estimation [21], which results in an ill-conditioned regressor matrix in (7). Also, recursive updates of $\widehat{H}^\alpha_{[k]}$ are desirable to capture changing operating points while reducing computational burden, and greater emphasis ought to be placed on more recent measurements than past ones that become outdated. Considering these circumstances, we use the recursive weighted partial least-squares (RWPLS) algorithm to compute $\widehat{H}^\alpha_{[k]}$, as it enhances OLS estimation for ill-posed regression problems.

Assuming that the per-area sensitivity models are updated every R samples, the RWPLS method employs the partial least-squares (PLS) decomposition recursively to project key components in $X^\alpha_{[k-R]}$ and $Y^\alpha_{[k-R]}$ onto lower-dimensional latent matrices $\Gamma^\alpha_{[k-R]}, G^\alpha_{[k-R]}, L^\alpha_{[k-R]}$. New design and response matrices $X^\alpha_{[k]}$ and $Y^\alpha_{[k]}$ at time step k can equivalently be represented by combining the PLS model of the previous estimation step at time step $k-R$ with newly collected measurements between time steps $k-R+1$ and k such that:

$$X^\alpha_{[k]} = \begin{bmatrix} \sigma G^\alpha_{[k-R]}{}^{\mathrm{T}} \\ \widehat{x}^\alpha_{[k-R+1]}{}^{\mathrm{T}} \quad 1 \\ \vdots \quad \vdots \\ \widehat{x}^\alpha_{[k]}{}^{\mathrm{T}} \quad 1 \end{bmatrix},\ Y^\alpha_{[k]} = \begin{bmatrix} \sigma \Gamma^\alpha_{[k-R]} L^\alpha_{[k-R]}{}^{\mathrm{T}} \\ \widehat{y}^\alpha_{[k-R+1]}{}^{\mathrm{T}} \\ \vdots \\ \widehat{y}^\alpha_{[k]}{}^{\mathrm{T}} \end{bmatrix}, \tag{8}$$

where the forgetting factor $\sigma \in (0, 1]$ prioritizes recent measurements over earlier ones. Finally, the estimated per-area sensitivity model $\widehat{H}^\alpha_{[k]}$ at time step k is obtained after decomposing $X^\alpha_{[k]}$ and $Y^\alpha_{[k]}$ into $\Gamma^\alpha_{[k]}, G^\alpha_{[k]}, L^\alpha_{[k]}$ via PLS by

$$\widehat{H}^\alpha_{[k]} = (G^\alpha_{[k]}\ G^\alpha_{[k]}{}^{\mathrm{T}})^{-1} G^\alpha_{[k]} \Gamma^\alpha_{[k]}\ L^\alpha_{[k]}{}^{\mathrm{T}}. \tag{9}$$

Details on the RWPLS method can be found in [22].

Example 1 (Sensitivity Model Estimation)**.** To illustrate ideas introduced above, consider the IEEE 33-bus test system (see, e.g., [23]) with the one-line diagram shown in Fig. 2. As a

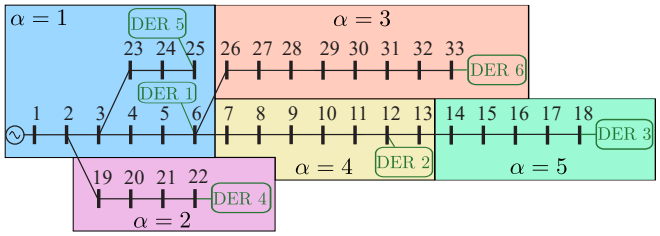

Fig. 2: IEEE 33-bus test system with DERs connected at arbitrarily chosen buses collected in $\mathcal{D} = \{6, 12, 18, 22, 25, 33\}$. The network is partitioned into five areas collected in the set $\mathcal{A} = \{1, 2, \ldots, 5\}$. Assume, without loss of generality, synchrophasor measurements are available at all buses. This test system is single phase, so $\mathcal{P}_i = \{a\}$, $\forall\ i \in \mathcal{N}$. As an example of the notation used throughout this paper, consider area 1. Within area 1, measured buses are collected in $\mathcal{E}^1 = \{1, 2, 3, 4, 5, 6, 23, 24, 25\}$ and buses connected to DERs are collected in $\mathcal{D}^1 = \{6, 25\}$. The extended set of buses is $\mathcal{E}^{1+} = \mathcal{E}^1 \cup \{7, 19, 26\}$. Adjacent areas are collected in $\mathcal{A}^1 = \{2, 3, 4\}$. Boundary buses are collected in $\mathcal{B}^1 = (\mathcal{E}^{1+} \cap \mathcal{E}^{2+}) \cup (\mathcal{E}^{1+} \cap \mathcal{E}^{3+}) \cup (\mathcal{E}^{1+} \cap \mathcal{E}^{4+}) = \{2, 6, 7, 19, 26\}$. Finally, the boundary bus 6 belongs to the extended set of buses in areas collected in $\mathcal{A}_6 = \{1, 3, 4\}$.

benchmark, we obtain the full-network sensitivity model H by evaluating the model-based power-flow Jacobian matrix at the operating point assuming an accurate network model is available. Next, we estimate the full-network sensitivity model $\widehat{H}$ using measurements obtained from all buses in the system. We also evaluate entries of the per-area sensitivity models using (9). For both full-network and per-area estimates, we collect 100 sets of measurements of bus voltage phase-angles and magnitudes and active- and reactive-power injections from synchrophasor measurements assumed to be available, without loss of generality, at all buses. Also assume that the active- and reactive-power components of loads at buses in $\mathcal{N} \setminus \{1\}$ vary randomly around their nominal values as Gaussian distributed random variables with 0 mean and 0.1% standard deviation relative to the respective nominal load values.

To assess the accuracy of the per-area sensitivity models, we reorder and stack the entries therein suitably to form a matrix comparable to the full-network sensitivity model. Using the Frobenius norm as an error metric, i.e., $||\widehat{H} - H||_F / ||H||_F$, we find that the full-network estimate has an error of 1.995×10^{-4}, compared to an error of 6.224×10^{-5} for the per-area estimate. The reason that the per-area sensitivity models yield lower estimation error than the full-network counterpart is as follows. Due to the sparse nature of the network connectivity, many entries in the sensitivity model are identically zero, but the full-network estimate contains very small nonzero values (all less than 0.035 in our numerical example). On the other hand, for the purpose of error comparison, we merge the per-area sensitivity models into the full-network analogue. In so doing, we make use of network connectivity information, i.e., the locations of zero entries. To illustrate the observations above, we plot heatmaps of the sensitivities in $J_{[k]}$ in Fig. 3. ■

IV. Distributed Optimal DER Dispatch

In this section, we formulate the optimal DER dispatch problem that embeds each per-area estimated sensitivity model as an equality constraint within the corresponding optimization subproblem. We also outline a tractable distributed solution approach using consensus-based ADMM algorithm.

A. Problem Formulation

We aim to determine the controllable DER active- and reactive-power setpoints in area $\alpha \in \mathcal{A}$ at time step $k+1$. Namely, we optimize over variables collected in vector $\overline{y}^{\alpha,\text{gen}}_{[k+1]} = [\{P^{\phi,\text{gen}}_{i,[k+1]}\}_{\phi\in\mathcal{P}_i, i\in\mathcal{D}^\alpha}, \{Q^{\phi,\text{gen}}_{i,[k+1]}\}_{\phi\in\mathcal{P}_i, i\in\mathcal{D}^\alpha}]^{\mathrm{T}}$, where $\mathcal{D}^\alpha$ denotes the set of buses with controllable DERs in area α. In turn, decision variables also include net injections and voltage phase-angles and magnitudes respectively collected in $\overline{y}^{\alpha}_{[k+1]} = [\{P^{\phi}_{i,[k+1]}\}_{\phi\in\mathcal{P}_i, i\in\mathcal{E}^\alpha}, \{Q^{\phi}_{i,[k+1]}\}_{\phi\in\mathcal{P}_i, i\in\mathcal{E}^\alpha}]^{\mathrm{T}}$ and $\overline{x}^{\alpha}_{[k+1]} = [\{\theta^{\phi}_{i,[k+1]}\}_{\phi\in\mathcal{P}_i, i\in\mathcal{E}^{\alpha+}}, \{V^{\phi}_{i,[k+1]}\}_{\phi\in\mathcal{P}_i, i\in\mathcal{E}^{\alpha+}}]^{\mathrm{T}}$. Constraints imposed on $\overline{x}^{\alpha}_{[k+1]}$, $\overline{y}^{\alpha}_{[k+1]}$, and $\overline{y}^{\alpha,\text{gen}}_{[k+1]}$ account for various operating ranges such as minimum and maximum allowable voltage limits and DER operating regions. Then, we pose the following separable optimization problem:

$$\underset{\substack{\overline{x}^\alpha, \overline{y}^\alpha, \overline{y}^{\alpha,\text{gen}},\\ \alpha\in\mathcal{A}}}{\text{minimize}} \ \sum_{\alpha\in\mathcal{A}} f^\alpha(\overline{x}^\alpha, \overline{y}^\alpha, \overline{y}^{\alpha,\text{gen}}) \tag{10a}$$

$$\text{subject to } \overline{y}^\alpha = J^\alpha_{[k]}\overline{x}^\alpha + c^\alpha_{[k]},\ \forall\,\alpha\in\mathcal{A}, \tag{10b}$$

$$x^\alpha_{\min} \le \overline{x}^\alpha \le x^\alpha_{\max},\ \forall\,\alpha\in\mathcal{A}, \tag{10c}$$

$$\overline{y}^{\alpha,\text{gen}} \in \mathcal{Y}^{\alpha,\text{gen}},\ \forall\,\alpha\in\mathcal{A}, \tag{10d}$$

$$\overline{y}^\alpha = \overline{y}^\alpha_{[k]} + C^\alpha(\overline{y}^{\alpha,\text{gen}} - y^{\alpha,\text{gen}}_{[k]}),\ \forall\,\alpha\in\mathcal{A}, \tag{10e}$$

$$z^\alpha_i = F^\alpha_i \overline{x}^\alpha = z_i,\ \forall\, i\in\mathcal{B}^\alpha, \alpha\in\mathcal{A}, \tag{10f}$$

where the parameterization of decision variables with respect to $k+1$ is dropped to contain notational burden. In (10e), C^α, $\alpha \in \mathcal{A}$, is the matrix that maps the DER bus/phase indices to buses/phases from which measurements are obtained in area α. Furthermore, (10f) represent consensus constraints that enforce voltage phase-angles and magnitudes at boundary buses shared among adjacent areas to be equal. To this end, we use matrix F^α_i, $\alpha \in \mathcal{A}$, to map voltage phase-angles and magnitudes in all phases of bus $i \in \mathcal{B}^\alpha$ in $\overline{x}^\alpha$ to auxiliary variable z_i, which is common for all areas with bus i as a boundary bus. The quadratic cost function in (10) is fully separable among different areas. It comprises a weighted sum of: (i) voltage phase-angle and magnitude deviations from respective references, (ii) nodal active- and reactive-power injection deviations from desired values, and (iii) cost of DER active- and reactive-power outputs, i.e.,

$$\begin{aligned} f^\alpha(\overline{x}^\alpha, \overline{y}^\alpha, \overline{y}^{\alpha,\text{gen}}) = {} & (\overline{x}^\alpha - x^{\alpha\circ})^{\mathrm{T}}\Psi^\alpha(\overline{x}^\alpha - x^{\alpha\circ}) \\ & + (\overline{y}^\alpha - y^{\alpha\circ})^{\mathrm{T}}\Phi^\alpha(\overline{y}^\alpha - y^{\alpha\circ}) \\ & + (\overline{y}^{\alpha,\text{gen}})^{\mathrm{T}}\Upsilon^\alpha\overline{y}^{\alpha,\text{gen}}, \end{aligned} \tag{11}$$

where $\overline{x}^{\alpha\circ}$ and $\overline{y}^{\alpha\circ}$, respectively, denote the voltage references and desired values for power injections at measured buses in area $\alpha \in \mathcal{A}$. In (11), $\Psi^\alpha = \text{diag}(\psi_1, \ldots, \psi_{2|\mathcal{E}^{\alpha+}|})$, $\Phi^\alpha = \text{diag}(\varphi_1, \ldots, \varphi_{2|\mathcal{E}^\alpha|})$, and $\Upsilon^\alpha = \text{diag}(\upsilon_1, \ldots, \upsilon_{2|\mathcal{D}^\alpha|})$ are diagonal matrices with non-negative entries, i.e.,

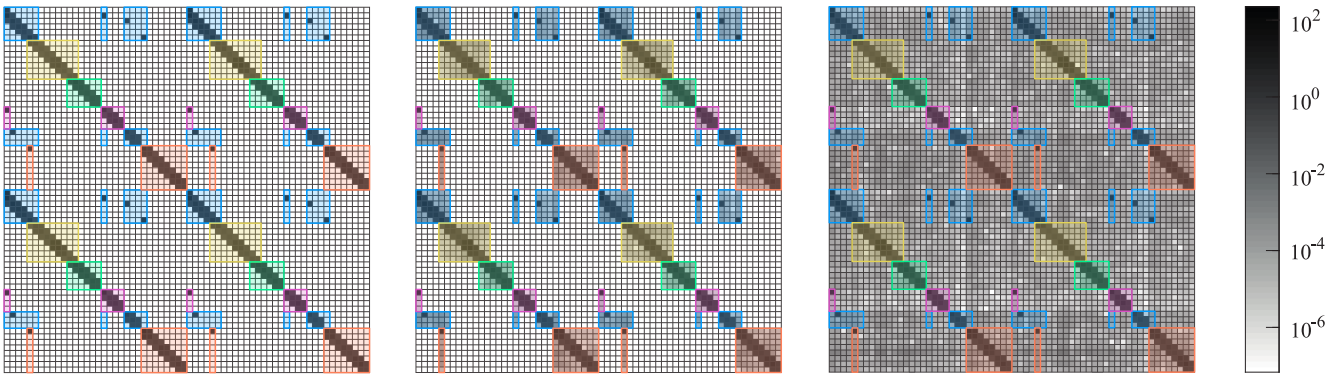

(a) (b) (c)

Fig. 3: Heatmap representations of the entries in $J_{[k]}$ for (a) the model-based sensitivities, (b) the measurement-based sensitivities from the proposed per-area estimation, and (c) the measurement-based sensitivities from the centralized estimation. Darker shades (approaching black) represent entries with larger magnitude, and the shade lightens with decreasing magnitude with white colour representing entries that are precisely zero. Shaded boxes delineate entries that are related to different areas, and colours used are consistent with those in Fig. 2.

$\psi_i, \varphi_i, \upsilon_i \geq 0$. Without loss of generalization, we assume that area 1 contains the substation bus 1. Note that $\overline{y}^{1}_{[k+1]}$ includes the substation power injections so that we can achieve feeder-level active- and reactive-power regulation. Before delving into the solution approach, we emphasize that the separable problem in (10) is *equivalent* to the problem in (2). Furthermore, as demonstrated in Example 1, the per-area estimated sensitivities $J^{\alpha}_{[k]}, \alpha \in \mathcal{A}$, are in fact *more* accurate than the full-network counterpart. Thus, the solution of the separable problem does not compromise on optimality as compared to the centralized problem in (2).

We collect decision variables pertinent to area α in $\chi^{\alpha} = [(\overline{x}^{\alpha})^{\mathrm{T}}, (\overline{y}^{\alpha})^{\mathrm{T}}, (\overline{y}^{\alpha,\mathrm{gen}})^{\mathrm{T}}]^{\mathrm{T}}$ and further we define entries in and structures of Π^{α}, π^{α}, κ^{α}, $A^{\alpha}_{[k]}$, $b^{\alpha}_{[k]}$, and $\mathcal{X}^{\alpha}$ in Appendix A so that (10) is expressed by:

$$\underset{\substack{\chi^{\alpha},\ \alpha\in\mathcal{A},\\ z^{\alpha}_i, z_i,\ i\in\mathcal{B}^{\alpha},\alpha\in\mathcal{A}}}{\text{minimize}} \quad \sum_{\alpha\in\mathcal{A}} \frac{1}{2}(\chi^{\alpha})^{\mathrm{T}}\Pi^{\alpha}\chi^{\alpha} + (\pi^{\alpha})^{\mathrm{T}}\chi^{\alpha} + \kappa^{\alpha} \tag{12a}$$

$$\text{subject to} \quad A^{\alpha}_{[k]}\chi^{\alpha} = b^{\alpha}_{[k]}, \forall\, \alpha \in \mathcal{A}, \tag{12b}$$

$$\chi^{\alpha} \in \mathcal{X}^{\alpha}, \forall\, \alpha \in \mathcal{A}, \tag{12c}$$

$$z^{\alpha}_i = K^{\alpha}_i \chi^{\alpha} = z_i, \forall\, i \in \mathcal{B}^{\alpha}, \alpha \in \mathcal{A}, \tag{12d}$$

where Π^{α} and π^{α} appropriately collect the quadratic and linear weights of the cost function in (11), and κ^{α} is a constant term that does not affect the problem solution. For area $\alpha \in \mathcal{A}$, the equality constraints in (10b) and (10e) collectively form (12b) with matrix $A^{\alpha}_{[k]}$ and vector $b^{\alpha}_{[k]}$ appropriately defined. Similarly, the set constraints in (10c) and (10d) are collectively rewritten as (12c), where $\mathcal{X}^{\alpha}$, $\alpha \in \mathcal{A}$, denotes the typically convex set of allowable DER operating regions as well as bus voltage bounds in area α. Finally, (12d) corresponds to consensus constraints in (10f), where K^{α}_i, $\alpha \in \mathcal{A}$, is a matrix containing 0s and 1s that maps voltage phase-angles and magnitudes of bus i in χ^{α} to z^{α}_i. Also, voltage phase-angle and magnitude of each boundary bus $i \in \mathcal{B}^{\alpha}$ are associated with auxiliary consensus variable z_i, coupled across areas that share bus i as a boundary bus, i.e., areas in the set $\mathcal{A}_i$.

With positive semidefinite weights in Π^{α}, (12) can be decomposed into $|\mathcal{A}|$ per-area convex quadratic subproblems coupled with consensus constraints pertinent to adjacent areas. Due to the consensus constraints among adjacent areas in (12d), standard solvers for the subproblems are not immediately applicable. In the next section, we present a tractable consensus-based ADMM algorithm to solve the DER dispatch problem in (12) in a distributed fashion, where only voltage phase-angles and magnitudes of boundary buses need to be exchanged among adjacent areas.

B. ADMM-based Solution Approach

The general idea of the distributed ADMM-based approach is to treat each per-area subproblem as a convex quadratic program. In addition, using the auxiliary variables defined for the voltage phase-angle and magnitude for each boundary bus, consensus among adjacent areas can be achieved. We decompose the problem in (12) for each area $\alpha \in \mathcal{A}$:

$$\underset{\substack{\chi^{\alpha},\omega^{\alpha},\\ z^{\gamma}_i, z_i, i\in\mathcal{B}^{\alpha},\gamma\in\mathcal{A}_i}}{\text{minimize}} \quad \frac{1}{2}(\chi^{\alpha})^{\mathrm{T}}\Pi^{\alpha}\chi^{\alpha} + (\pi^{\alpha})^{\mathrm{T}}\chi^{\alpha} \tag{13a}$$

$$\text{subject to} \quad A^{\alpha}_{[k]}\chi^{\alpha} = b^{\alpha}_{[k]}, \tag{13b}$$

$$\omega^{\alpha} \in \mathcal{X}^{\alpha}, \tag{13c}$$

$$\omega^{\alpha} = \chi^{\alpha}, \tag{13d}$$

$$z^{\gamma}_i - z_i = 0,\ \forall\, i \in \mathcal{B}^{\alpha}, \gamma \in \mathcal{A}_i, \tag{13e}$$

$$z^{\alpha}_i = K^{\alpha}_i \chi^{\alpha},\ \forall\, i \in \mathcal{B}^{\alpha}, \tag{13f}$$

where we define auxiliary variables ω^{α} and tie it to decision variables χ^{α} with the equality constraint in (13d), and $\gamma \in \mathcal{A}_i$ is a dummy index variable. Notably, in (13), the per-area equality constraints on χ^{α}, per-area bound constraints on χ^{α}, and consensus constraints among adjacent areas are each associated with a different decision variable.

For the per-area subproblem, the ADMM algorithm alternates between solving an equality-constrained quadratic program with a projection onto feasible bound constraints, while achieving consensus among areas via (13e). The augmented Lagrangian associated with (13) is given by

$$\begin{aligned}&\mathcal{L}_\rho^\alpha(\chi^\alpha,\omega^\alpha,\mu^\alpha,\{z_i^\gamma,z_i,s_i^\gamma\}_{i\in\mathcal{B}^\alpha,\gamma\in\mathcal{A}_i})\\&=\Big(\frac{1}{2}(\chi^\alpha)^{\mathrm{T}}\Pi^\alpha\chi^\alpha+(\pi^\alpha)^{\mathrm{T}}\chi^\alpha\\&\quad+\frac{\rho}{2}\left\|\chi^\alpha-\omega^\alpha+\mu^\alpha\right\|_2^2-\frac{\rho}{2}\left\|\mu^\alpha\right\|_2^2\Big)\\&\quad+\sum_{i\in\mathcal{B}^\alpha}\sum_{\gamma\in\mathcal{A}_i}\frac{\rho}{2}\big(||z_i^\gamma-z_i+s_i^\gamma||_2^2-||s_i^\gamma||_2^2\big),\end{aligned}\tag{14}$$

where ρ is a positive scalar ADMM parameter, μ^α, and s_i^γ are scaled dual variables for the coupling constraints (13d) and (13e). Note that we do not include constraints (13b), (13c) and (13f) in the augmented Lagrangian as they will be considered in the respective subproblems. Below, we provide a brief summary of the iterative algorithm, which is later used in numerical case studies presented in Section V. The ADMM algorithm uses a sequence of iterations indexed by ℓ to search for the optimizer of (13).

The primal variable update for area $\alpha\in\mathcal{A}$ solves for $(\chi^\alpha)^{\ell+1}$ and $(z_i^\alpha)^{\ell+1}$ from the following standard equality-constrained convex quadratic program:

$$\begin{aligned}\underset{\chi^\alpha,z_i^\alpha,\ i\in\mathcal{B}^\alpha}{\text{minimize}}\quad&\frac{1}{2}(\chi^\alpha)^{\mathrm{T}}\Pi^\alpha\chi^\alpha+(\pi^\alpha)^{\mathrm{T}}\chi^\alpha\\&+\frac{\rho}{2}\left\|\chi^\alpha-(\omega^\alpha)^\ell+(\mu^\alpha)^\ell\right\|_2^2\\&+\sum_{i\in\mathcal{B}^\alpha}\frac{\rho}{2}\left\|z_i^\alpha-(z_i)^\ell+(s_i^\alpha)^\ell\right\|_2^2\end{aligned}\tag{15a}$$

$$\text{subject to}\quad A_{[k]}^\alpha\chi^\alpha=b_{[k]}^\alpha,\tag{15b}$$

$$z_i^\alpha=K_i^\alpha\chi^\alpha,\ \forall\, i\in\mathcal{B}^\alpha.\tag{15c}$$

The solution to (15) can be readily obtained via a closed-form solution [24]. Next, armed with the primal updates for iteration $\ell+1$, the updates for auxiliary variables ω^α and z_i, $i\in\mathcal{B}^\alpha$, are respectively given by

$$(\omega^\alpha)^{\ell+1}=\arg\underset{\omega^\alpha\in\mathcal{X}^\alpha}{\text{minimize}}\frac{\rho}{2}||(\chi^\alpha)^{\ell+1}-\omega^\alpha+(\mu^\alpha)^\ell||_2^2,\tag{16}$$

$$(z_i)^{\ell+1}=\arg\underset{z_i}{\text{minimize}}\sum_{\gamma\in\mathcal{A}_i}\frac{\rho}{2}||(z_i^\gamma)^{\ell+1}-z_i+(s_i^\gamma)^\ell||_2^2.\tag{17}$$

The projection problem in (16) admits closed-form solutions for voltage bounds and typical constraints on DER outputs [24]. Specifically, for the projection onto independent active- and reactive-power box limits, the solution to (16) is

$$(\omega^\alpha)^{\ell+1}=\min(\chi_{\max}^\alpha,\max(\chi_{\min}^\alpha,(\chi^\alpha)^{\ell+1}-(\mu^\alpha)^\ell)),\tag{18}$$

where $\chi_{\min}^\alpha$ and $\chi_{\max}^\alpha$ comprise, respectively, the entry-wise lower and upper bounds of χ^α. Closed-form projections onto other typical DER operational regions are provided in [2] and can be readily integrated in the proposed ADMM solution approach. For the auxiliary variable z_i, $i\in\mathcal{B}^\alpha$, the problem in (17) solves as the average of $(z_i^\gamma)^{\ell+1}$, $\gamma\in\mathcal{A}_i$, i.e., [25]

$$(z_i)^{\ell+1}=\frac{1}{|\mathcal{A}_i|}\sum_{\gamma\in\mathcal{A}_i}(z_i^\gamma)^{\ell+1}.\tag{19}$$

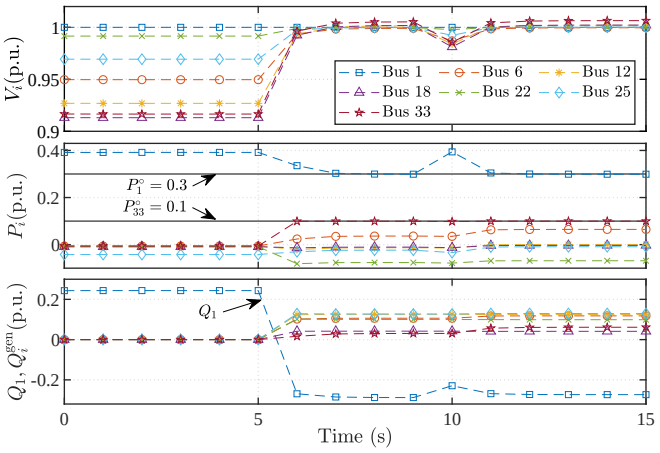

Fig. 4: Time-domain simulation via proposed distributed measurement-based optimal DER dispatch when DERs are activated at time $t_{\text{start}}=5\,\text{s}$, and at time $t_\Delta=10\,\text{s}$, the system operating point is changed. Top pane: bus voltages V_i at buses with DERs; Middle pane: bus active-power injections P_i at buses with DERs; Bottom pane: substation reactive-power injection Q_1 and DER reactive-power injections Q_i^{gen} at buses with DERs.

Finally, the scaled dual variables admit straightforward recursive updates given by

$$(\mu^\alpha)^{\ell+1}=(\mu^\alpha)^\ell+(\omega^\alpha)^{\ell+1}-(\chi^\alpha)^{\ell+1},\tag{20}$$

$$(s_i^\alpha)^{\ell+1}=(s_i^\alpha)^\ell+(z_i)^{\ell+1}-(z_i^\alpha)^{\ell+1}.\tag{21}$$

The ADMM algorithm outlined above repeatedly updates primal variables via (15), followed by the auxiliary variables via (16) and (17) and dual variables via (20) and (21) until: $||(\chi^\alpha)^\ell-(\omega^\alpha)^\ell||_2+||\{(z_i^\alpha)^\ell-(z_i)^\ell\}_{i\in\mathcal{B}^\alpha}||_2<\epsilon$ and $||\rho((\omega^\alpha)^\ell-(\omega^\alpha)^{\ell-1})||_2+||\rho(\{(z_i)^\ell-(z_i)^{\ell-1}\}_{i\in\mathcal{B}^\alpha})||_2<\epsilon$, for some predefined tolerance $\epsilon>0$. We initialize auxiliary variables $(\omega^\alpha)^0$ and $(z_i)^0$ with values corresponding to the operating point at time step k just before optimization, and set initial conditions for primal and scaled dual variables to 0. The ADMM iterations continue until the stopping criteria are satisfied with optimizer given by $\chi^{\alpha\star}$ from which optimal DER dispatch $\overline{y}^{\alpha,\text{gen}\star}$ (i.e., $P_i^{\alpha,\text{gen}\star}$ and $Q_i^{\alpha,\text{gen}\star}$, $i\in\mathcal{D}^\alpha$) can be extracted. We highlight that all the updates of primal and dual variables can be computed in parallel via closed-form solutions for each area $\alpha\in\mathcal{A}$. The only step that requires exchange among the areas is the auxiliary variable update in (19), in which updated voltage phase-angles and magnitudes at boundary buses are shared among adjacent areas.

Example 2 (Distributed Optimal DER Dispatch)**.** We present simulation results of the distributed optimal DER dispatch method outlined above as compared to the centralized version in [15]. We assume that DERs are connected to buses in the set $\mathcal{D}=\{6,12,18,22,25,33\}$, as depicted in Fig. 2. The DER active- and reactive-power setpoints are dispatched to simultaneously (i) minimize voltage-magnitude deviations from reference level of 1 p.u., (ii) regulate active-power injections at buses 1 and 33 to desired values of 0.3 p.u. and

TABLE I: Comparison of cost-function and relative-errors among (i) the centralized model-based nonlinear DER dispatch, (ii) the centralized measurement-based DER dispatch, and (iii) the proposed distributed measurement-based DER dispatch.

	Cost function (p.u.)	Cost function error (%)	Voltage-magnitude error (%)	Active-power error (%)	Reactive-power error (%)
Model-based (Central)	0.0077	—	—	—	—
Meas-based (Central)	0.0077	0.054	0.002	5.800	0.939
Meas-based (Dist)	0.0077	0.054	0.002	5.849	0.067

0.1 p.u., respectively, and (iii) minimize cost of DER active- and reactive-power outputs.

In Fig. 4, we plot time evolution of voltage magnitudes and active-power injections at DER buses, as well as DER and substation reactive-power outputs. The system initially operates without DER participation. The DERs are activated at time $t_{\text{start}} = 5\,\text{s}$. Subsequently, at time $t_{\Delta} = 10\,\text{s}$, the system operating point changes as active- and reactive-power loads at all buses in the system increase by 25%. Simulations run until time $t_{\text{end}} = 15\,\text{s}$. Once DERs are activated at time $t_{\text{start}} = 5\,\text{s}$, we observe that the proposed measurement-based dispatch effectively achieves the weighted objectives of minimizing voltage-magnitude deviations from 1 p.u. and regulating the active-power injections at buses 1 and 33 to their respective setpoints. After the operating-point change at time $t_{\Delta} = 10\,\text{s}$, the proposed method updates the linear sensitivity models and adapts the DER dispatch to achieve the same objectives.

We benchmark the proposed distributed measurement-based optimal DER dispatch method against centralized model- and measurement-based analogues, where all buses in the network are assumed to belong to one area. The nonlinear model-based optimal dispatch problem is solved with the MATPOWER Interior Point Solver [26]. We record voltage profiles and bus active- and reactive-power injections, at $t_{\text{end}} = 15\,\text{s}$ for (i) the centralized model-based nonlinear DER dispatch, (ii) the centralized measurement-based DER dispatch, and (iii) the proposed distributed measurement-based DER dispatch. Table I summarizes errors in (ii) and (iii) as compared to the model-based benchmark (i). The converged solution from the proposed method indeed matches very closely to those from model-based optimal dispatch with accurate system model and the centralized measurement-based dispatch, with respect to the cost function value, voltage magnitudes, and active- and reactive-power injections. ■

V. Application to Multi-phase System

In this section, we demonstrate the scalability of the proposed distributed measurement-based optimal DER dispatch framework via numerical case studies involving the IEEE 123-bus test system shown in Fig. 5. We refer interested readers to [27] for details on system parameters.

A. Simulation Setup

We use residential customer load profiles for a 24-hour period with 1-min resolution from [6], that we interpolate to obtain 1-second resolution load data. A random number of customers (integer between 5 and 10) is connected to load

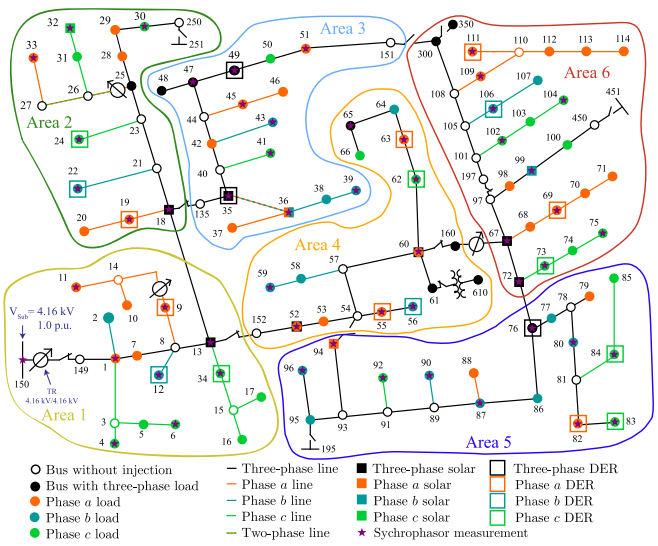

Fig. 5: IEEE 123-bus multi-phase test system partitioned into 6 areas. Synchrophasor measurements are available at 60% of buses with load and/or generation, DERs are installed at 25% of buses.

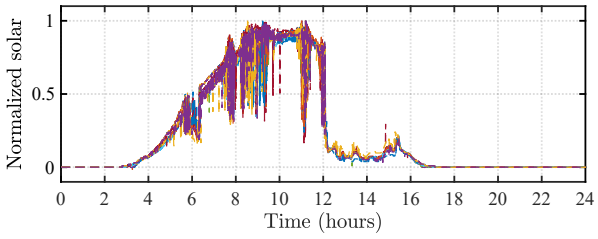

Fig. 6: Normalized daily solar PV output for different locations with intermittent solar irradiation [28].

buses, resulting in non-uniform distribution of loads across different phases. We assume a constant power factor of 95% for each load. We also connect uncontrolled three-phase solar photovoltaic (PV) systems at buses $13, 18, 35, 52, 60, 67, 72$, single-phase solar at buses $32c$, $94a$, and $99b$, and two-phase solar at bus 36 between phases a and b. The solar PV output is normalized from actual measurements with 1-second resolution [28], and each solar PV system uses a different profile from the data set, as shown in Fig. 6. We use solar PV profiles from a day with rapid fluctuations and high ramp rates in generation before noon, which challenge the model estimation and optimal dispatch.

We partition the test system into 6 areas, with each containing several single- and three-phase DERs, as indicated in Fig. 5. The DERs operate with independent active- and reactive-power limits within $P_i^{\text{gen}} \in [-0.05, 0.05]$ p.u. and $Q_i^{\text{gen}} \in [-0.05, 0.05]$ p.u. Three-phase DERs operate in balanced manner, where active- and reactive-power outputs are equal across all phases. In the simulations, we deactivate existing voltage regulators as DERs are used to regulate voltages and we limit our studies to the default switch configurations.

In three different scenarios, we assume that measurements of voltage phasors and active- and reactive-power injections sampled at 1-second intervals are available from (i) all area boundary buses as well as locations with controllable DERs

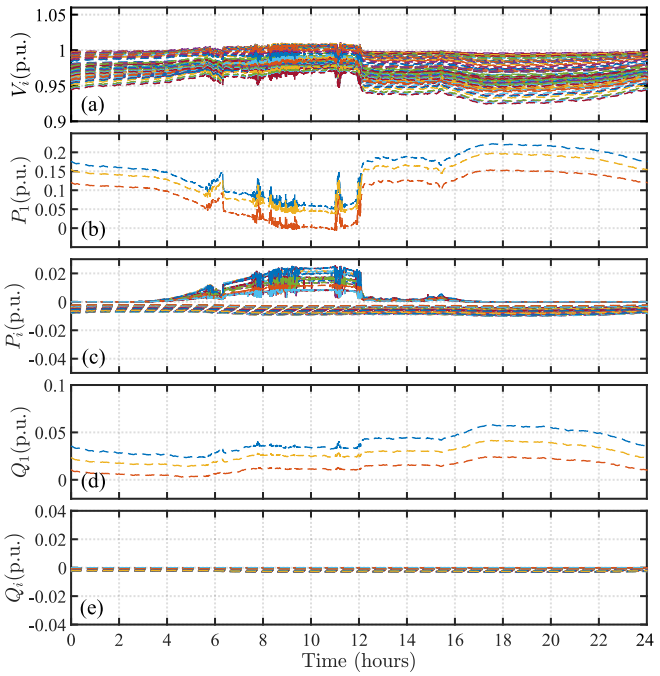

Fig. 7: Time-domain simulation of the scenario without active DER control. (a) bus voltages V_i at all buses; (b) substation active-power injections P_1; (c) bus active-power injections P_i at buses with loads/injections; (d) substation reactive-power injections Q_1; (e) bus reactive-power injections Q_i at buses with loads/injections.

resulting in a synchrophasor measurement coverage of 40%, (ii) buses labelled with $\star$ in Fig. 5 resulting in a synchrophasor measurement coverage of 60%, and (iii) from all buses in the system corresponding to 100% synchrophasor measurement coverage.

The sensitivity model for each area is updated every $R = 10$ samples via RWPLS in (9). Optimal DER dispatch is similarly solved every 10 seconds to allow ample time for the ADMM-based solution to converge to the new setpoints. We dispatch DER active- and reactive-power setpoints to simultaneously (i) regulate the active- and reactive-power injections at the substation bus 1 to 0.15 and 0.03 p.u., respectively, and (ii) minimize cost of DER active- and reactive-power outputs while keeping voltages within acceptable bounds of 0.95 and 1.05 p.u. We set entries in the diagonal weight matrices Ψ, Φ, and Υ accordingly to achieve the objective above.

B. Discussion of Simulation Results

In this subsection, we evaluate the performance of the proposed method and discuss the simulation results. In particular, we evaluate (i) time-domain evolution of bus voltage magnitudes as well as active- and reactive-power injections, (ii) performance of different levels of synchrophasor measurement coverage, and (iii) execution times.

1) Time-domain Evolution: In Figs. 7 and 8, respectively, for the cases without and with DER control via the distributed measurement-based framework, we plot time evolution of bus voltage magnitudes at all buses with load and/or generation, as well as active- and reactive-power injections at the substation and at buses with DERs for the scenario with 60% synchrophasor measurement coverage. In Fig. 8, we observe that the substation active- and reactive-power injections are indeed regulated to their respective references and voltages are regulated within the acceptable bounds of 0.95 and 1.05 p.u. The proposed framework is very effective during times with relatively smooth solar PV output, but it is challenged under highly intermittent conditions, where the operational objectives are not met with the 10-second DER setpoint updates. This issue may be addressed by pairing the proposed method with local DER controllers or by reducing the time between consecutive DER setpoint updates. We emphasize that the 60% synchrophasor coverage is by no means a requirement for the proposed method to be effective. It simply reflects a future scenario with widespread measurement coverage due, in part, to greater DER integration. Such a scenario calls for distributed algorithms, like the one proposed in this paper, that can be implemented at scale.

2) Comparison of Different Synchrophasor Coverage: We compare the probability of various bus voltage values for the three scenarios with different levels of synchrophasor measurement coverage. Particularly, in Fig. 9, we plot histograms of all bus voltages during the 24-hour simulation period for the three scenarios of 40%, 60%, and 100% synchrophasor measurement coverage, compared to the case without active DER control. For the three scenarios of 40%, 60%, and 100%, respectively, 99.20%, 99.83%, and 99.95% of the bus voltages are within voltage limits of 0.95 p.u. and 1.05 p.u. Without DER support, voltage violations occur more frequently, 94.52% of the bus voltages are within limits over the simulation time. Further, we evaluate the probability of voltage violations at the bus with the lowest voltage in the system (bus 114) in Fig. 10. We observe that the probability of voltage violations is reduced, when synchrophasor measurements are available at a higher share of the buses. For the case with partial synchrophasor coverage of 40% and 60%, we obtain a probability of voltage violations below 0.95 p.u. of 88.75% and 59.7% as compared to 9.05% for the case with full coverage. This is because with partial synchrophasor coverage, voltage violations at unobserved buses are not accounted for in the optimal DER dispatch. Nevertheless, in all three scenarios with active DER control, the voltage violations are only of small magnitudes up to 0.005 p.u. In contrast, without active DER control, there are significant voltage violations up to 0.025 p.u. during the majority of the day. These results suggest that even partial synchrophasor coverage significantly benefits the operational performance, and the case with full coverage improves the performance even more.

3) Execution Time: In Table II, we highlight the computational benefits of the distributed method by reporting execution times required for model estimation via RWPLS and DER dispatch via distributed ADMM-based optimization for 3 scenarios with different levels of synchrophasor measurement coverage. We compare these to the centralized implementation from [15]. We implement pertinent algorithms in MATLAB R2018b on a personal computer with Intel Core i7-10610U processor at 1.80 GHz, and 16 GB RAM. For the

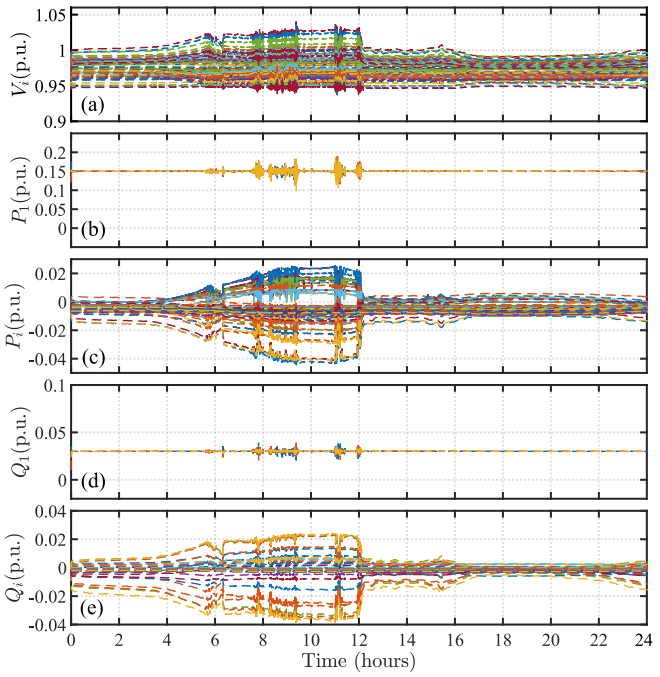

Fig. 8: Time-domain simulation via proposed estimation and optimization framework. (a) bus voltages V_i at all buses; (b) substation active-power injections P_1; (c) bus active-power injections P_i at buses with loads/injections; (d) substation reactive-power injections Q_1; (e) bus reactive-power injections Q_i at buses with loads/injections.

TABLE II: Comparison of execution times.

Synchrophasor Coverage		Model Estimation (s)	Optimal DER Dispatch Per iteration (s)	# iterations	Total (s)
40%	Centralized	0.499	3.906×10^{-5}	2245	0.094
	Distributed	0.0062	1.567×10^{-5}	1120	0.0176
60%	Centralized	1.216	4.783×10^{-5}	2739	0.131
	Distributed	0.0098	2.023×10^{-5}	1246	0.0252
100%	Centralized	1.924	1.586×10^{-4}	3122	0.495
	Distributed	0.021	2.608×10^{-5}	1484	0.0387

distributed method, we report execution times for area 6, as it contains the most measurement locations and DERs. We set the ADMM parameter $\rho = 0.7$ and the residual tolerance $\epsilon = 10^{-6}$. These parameters are set empirically to achieve good convergence and satisfactorily accurate DER setpoints. We observe computational savings in the scenarios with partial synchrophasor coverage over the one with full coverage, due to lower-dimensional estimation and optimization problems. In the scenarios with 60% and 100% synchrophasor coverage, the centralized implementation of the estimation and optimization tasks exceeds the 1-s interval between consecutive measurement samples, limiting practical applicability. On the other hand, in our particular implementation, the proposed distributed method overcomes scalability issues with around $100\times$ and $10\times$ improvements in model estimation and optimization tasks, respectively, thus facilitating real-time operations.

4) Communication Considerations: In both the estimation and optimization stages, the only information that needs to be communicated between two adjacent areas are variables associated with the boundary buses that are connected across

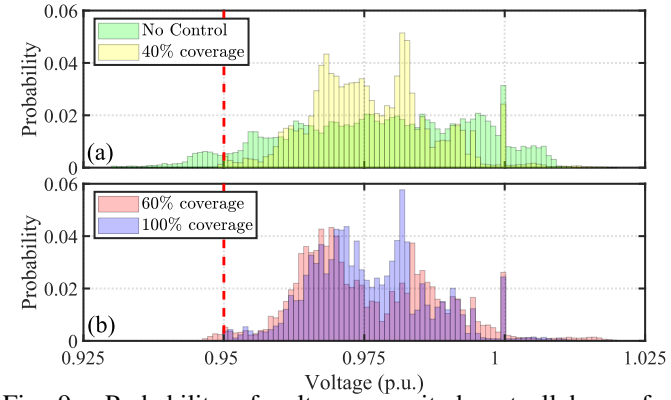

Fig. 9: Probability of voltage magnitudes at all buses for the different simulation scenarios. (a) Scenario without active DER control and scenario with active DER control and 40% synchrophasor measurement coverage; (b) Scenarios with active DER control with 60% and 100% synchrophasor measurement coverage, respectively. The vertical red line indicates the lower voltage limit of 0.95 p.u.

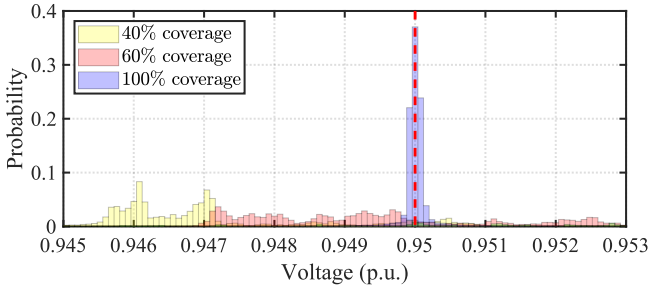

Fig. 10: Probability of bus voltage violations at bus 114 with different levels of synchrophasor measurement coverage of 40%, 60%, and 100%. The vertical red line indicates the lower voltage limit of 0.95 p.u.

the two areas, not those associated with internal buses. Also, since information is only required of neighbouring buses in adjacent areas, the physical distance over which data is transferred is relatively small. Moreover, while ADMM requires many iterations when the stopping criterion imposes a tight tolerance, it can lead to good performance in a fraction of the number of iterations [25]. For example, we set $\epsilon = 10^{-6}$ for the execution times reported in Table II. On the other hand, if we set $\epsilon = 10^{-3}$, in the 100% coverage case, it takes merely 68 iterations (instead of 1484) for the ADMM to converge to DER setpoints that achieve an objective function value only 1.6429×10^{-5}% higher than that achieved by setting $\epsilon = 10^{-6}$. With modern communication channels like 5G offering round-trip communication times in the range of 1 ms [29], the communication delay would incur approximately an additional 0.07 s on the execution time.

VI. Concluding Remarks

In this paper, we present a distributed measurement-based method to dispatch optimal DER active- and reactive-power outputs that adapt to system operating point. Optimal DER setpoints are obtained by embedding recursively estimated per-area sensitivity models as equality constraints in an optimiza-

tion problem, which is solved in distributed fashion via the consensus-based ADMM method. The distributed estimation and optimization require little information exchange among adjacent areas (only voltages at boundary buses) and yield closed-form solutions. As demonstrated by numerical case studies, the main advantages of the proposed method include (i) adaptability to operating-point changes, (ii) computational savings over centralized implementations in both the model estimation and optimal DER dispatch, and (iii) requiring only information about which areas are adjacent to its boundary buses from an offline network topology model. Finally, important avenues for future research include application of ADMM-based algorithms that mitigate against communication noise or failure (see e.g., [30], [31]) and consideration of DERs with nonconvex operating regions.

APPENDIX

A. Reformulating (10) and (11) as Quadratic Program in (12)

In (12), Π^α, π^α, and κ^α are obtained by suitable algebraic manipulations of (11) and they are given by

$$\Pi^\alpha = 2\begin{bmatrix}\Psi^\alpha & 0 & 0\\ 0 & \Phi^\alpha & 0\\ 0 & 0 & \Upsilon^\alpha\end{bmatrix}, \quad \pi^\alpha = -2\begin{bmatrix}\Psi^\alpha x^{\alpha\circ}\\ \Phi^\alpha y^{\alpha\circ}\\ 0\end{bmatrix}, \tag{22}$$

$$\kappa^\alpha = (x^{\alpha\circ})^{\mathrm{T}}\Psi x^{\alpha\circ} + (y^{\alpha\circ})^{\mathrm{T}}\Phi y^{\alpha\circ}, \tag{23}$$

where 0s are matrices or vectors of all zeros with appropriate dimension. The linear constraints in (12b) is constructed by combining (10b) and (10e) with

$$A^\alpha_{[k]} = \begin{bmatrix}-J^\alpha_{[k]} & I_{2|\mathcal{E}^\alpha|} & 0\\ 0 & I_{2|\mathcal{E}^\alpha|} & -C^\alpha\end{bmatrix}, \; b^\alpha_{[k]} = \begin{bmatrix}c^\alpha_{[k]}\\ \overline{y}^\alpha_{[k]} - C^\alpha \overline{y}^{\alpha,\mathrm{gen}}_{[k]}\end{bmatrix}, \tag{24}$$

where $I_{2|\mathcal{E}^\alpha|}$ denotes the $2|\mathcal{E}^\alpha| \times 2|\mathcal{E}^\alpha|$ identity matrix and 0s represent matrices of all zeros with appropriate dimensions. Finally, $\mathcal{X}^\alpha$ represents the composition of set constraints in (10c) and (10d).

REFERENCES

[1] IRENA (2019), "Innovation landscape brief: Market integration of distributed energy resources," *International Renewable Energy Agency*, 2019.

[2] E. Dall'Anese and A. Simonetto, "Optimal power flow pursuit," *IEEE Trans. Smart Grid*, vol. 9, no. 2, pp. 942–952, Mar. 2018.

[3] A. von Meier, E. Stewart, A. McEachern, M. Andersen, and L. Mehrmanesh, "Precision micro-synchrophasors for distribution systems: a summary of applications," *IEEE Trans. Smart Grid*, vol. 8, no. 6, pp. 2926–2936, Nov. 2017.

[4] C. Mugnier, K. Christakou, J. Jaton, M. De Vivo, M. Carpita, and M. Paolone, "Model-less/measurement-based computation of voltage sensitivities in unbalanced electrical distribution networks," in *Proc. of Power Syst. Comp. Conf.*, Jun. 2016.

[5] Y. C. Chen, J. Wang, A. D. Domínguez-García, and P. W. Sauer, "Measurement-based estimation of the power flow Jacobian matrix," *IEEE Trans. Smart Grid*, vol. 7, no. 5, pp. 2507–2515, Sep. 2016.

[6] O. Ardakanian, V. W. S. Wong, R. Dobbe, S. H. Low, A. von Meier, C. J. Tomlin, and Y. Yuan, "On identification of distribution grids," *IEEE Trans. Control Netw. Syst.*, vol. 6, no. 3, pp. 950–960, Sep. 2019.

[7] A. von Meier, "Synchrophasor monitoring for distribution systems: Technical foundations and applications," NASPI Distribution Task Team, Tech. Rep., Jan. 2018.

[8] V. Kekatos and G. B. Giannakis, "Distributed robust power system state estimation," *IEEE Trans. Power Syst.*, vol. 28, no. 2, pp. 1617–1626, Oct. 2013.

[9] H. Zhu and G. B. Giannakis, "Power system nonlinear state estimation using distributed semidefinite programming," *IEEE J. Sel. Topics Signal Process.*, vol. 8, no. 6, pp. 1039–1050, Jun. 2014.

[10] X. Zhou, Z. Liu, Y. Guo, C. Zhao, J. Huang, and L. Chen, "Gradient-based multi-area distribution system state estimation," *IEEE Trans. Smart Grid*, vol. 11, no. 6, pp. 5325–5338, Nov. 2020.

[11] H. Su, P. Li, P. Li, X. Fu, L. Yu, and C. Wang, "Augmented sensitivity estimation based voltage control strategy of active distribution networks with PMU measurement," *IEEE Access*, vol. 7, pp. 44 987–44 997, Mar. 2019.

[12] H. Xu, A. D. Domínguez-García, V. Veeravalli, and P. W. Sauer, "Data-driven voltage regulation in radial power distribution systems," *IEEE Trans. Power Syst.*, vol. 35, no. 3, pp. 2133–2143, May 2020.

[13] H. Xu, A. D. Domínguez-García, and P. W. Sauer, "Data-driven coordination of distributed energy resources for active power provision," *IEEE Trans. Power Syst.*, vol. 34, no. 4, pp. 3047–3058, Jul. 2019.

[14] M. D. Sankur, R. Dobbe, A. von Meier, and D. B. Arnold, "Model-free optimal voltage phasor regulation in unbalanced distribution systems," *IEEE Trans. Smart Grid*, vol. 11, no. 1, pp. 884–894, Jan. 2020.

[15] S. Nowak, Y. C. Chen, and L. Wang, "Measurement-based optimal der dispatch with a recursively estimated sensitivity model," *IEEE Trans. Power Syst.*, vol. 35, no. 6, pp. 4792–4802, Nov. 2020.

[16] S. Bolognani, R. Carli, G. Cavraro, and S. Zampieri, "On the need for communication for voltage regulation of power distribution grids," *IEEE Trans. Control Netw. Syst.*, vol. 6, no. 3, pp. 1111–1123, Sep. 2019.

[17] G. Qu and N. Li, "Optimal distributed feedback voltage control under limited reactive power," *IEEE Trans. Power Syst.*, vol. 35, no. 1, pp. 315–331, Jan. 2020.

[18] C. Chang, M. Colombino, J. Cort, and E. Dall'Anese, "Saddle-flow dynamics for distributed feedback-based optimization," *IEEE Control Syst. Lett.*, vol. 3, no. 4, pp. 948–953, Oct. 2019.

[19] A. Bernstein and E. Dall'Anese, "Real-time feedback-based optimization of distribution grids: A unified approach," *IEEE Trans. Control Netw. Syst.*, vol. 6, no. 3, pp. 1197–1209, Sep. 2019.

[20] D. K. Molzahn, F. Drfler, H. Sandberg, S. H. Low, S. Chakrabarti, R. Baldick, and J. Lavaei, "A survey of distributed optimization and control algorithms for electric power systems," *IEEE Trans. Smart Grid*, vol. 8, no. 6, pp. 2941–2962, Nov. 2017.

[21] J. Zhang, Z. Wang, X. Zheng, L. Guan, and C. Y. Chung, "Locally weighted ridge regression for power system online sensitivity identification considering data collinearity," *IEEE Trans. Power Syst.*, vol. 33, no. 2, pp. 1624–1634, Mar. 2018.

[22] S. J. Qin, "Recursive PLS algorithms for adaptive data modeling," *Computers & Chemical Engineering*, vol. 22, no. 4, pp. 503–514, Aug. 1998.

[23] M. E. Baran and F. F. Wu, "Network reconfiguration in distribution systems for loss reduction and load balancing," *IEEE Trans. Power Del.*, vol. 4, no. 2, pp. 1401–1407, Apr. 1989.

[24] A. U. Raghunathan and S. Di Cairano, "ADMM for convex quadratic programs: Q-linear convergence and infeasibility detection," *arXiv preprint arXiv:1411.7288*, Oct. 2014.

[25] S. Boyd, N. Parikh, and E. Chu, *Distributed optimization and statistical learning via the alternating direction method of multipliers*. Now Publishers Inc, 2011.

[26] R. D. Zimmerman, C. E. Murillo-Sánchez, and R. J. Thomas, "Matpower: steady-state operations, planning, and analysis tools for power systems research and education," *IEEE Trans. Power Syst.*, vol. 26, no. 1, pp. 12–19, Feb. 2011.

[27] W. H. Kersting, "Radial distribution test feeders," *IEEE Trans. Power Syst.*, vol. 6, no. 3, pp. 975–985, Aug. 1991.

[28] EPRI. (2012) Distributed PV monitoring and feeder analysis. [Online]. Available: https://dpv.epri.com/media/pvdata20120616-24-1-second.zip

[29] I. Parvez, A. Rahmati, I. Guvenc, A. I. Sarwat, and H. Dai, "A survey on low latency towards 5G: Ran, core network and caching solutions," *IEEE Commun. Surv. Tutor.*, vol. 20, no. 4, pp. 3098–3130, May 2018.

[30] L. Majzoobi, V. Shah-Mansouri, and F. Lahouti, "Analysis of distributed ADMM algorithm for consensus optimisation over lossy networks," *IET Signal Process.*, vol. 12, no. 6, pp. 786–794, Aug. 2018.

[31] L. Majzoobi, F. Lahouti, and V. Shah-Mansouri, "Analysis of distributed ADMM algorithm for consensus optimization in presence of node error," *IEEE Trans. Signal Process.*, vol. 67, no. 7, pp. 1774–1784, Jan. 2019.